

Investigating the biological and mechanical performance of cranberry-modified silicone materials for use in implantable medical devices

By Louis Briggs

Department of Chemical Engineering

McGill University, Montreal

August 2014

A thesis submitted to McGill University
in partial fulfillment of the requirements of the degree of
Master of Engineering

© Louis Briggs 2014

Abstract

Catheter associated urinary tract infections (CAUTIs) are the second most common type of hospital acquired infection in North America with over a million cases reported each year. This high incidence rate, together with the dissemination of antibiotic resistant uropathogens has resulted in much interest in the development of preventative measures within the research community. The consumption of *Vaccinium macrocarpon*, the North American cranberry, has been linked with the prevention of bacterial infections in the urinary tract for over 100 years. The McGill Biocolloids and Surfaces Laboratory has shown that cranberry derived materials (CDMs) can inhibit bacterial adherence to surfaces, impair bacterial motility, and influence various bacterial virulence functions. It is therefore hypothesized that cranberries and CDMs could prevent the development of CAUTIs via the disruption of various stages of pathogenesis. Herein, we report on the bioperformance of cranberry impregnated biomedical grade silicone against the biofilms formed by *Proteus mirabilis*, a clinically relevant uropathogen. In addition, the mechanical performance of this cranberry-silicone hybrid material is studied. First, the release of bioactive cranberry materials into an aqueous environment is demonstrated in lysogeny broth using a spectrophotometric method. Second, the ultimate tensile strength, elongation at break, storage modulus, and contact angle of CDM impregnated silicone are reported. Finally, the ability of *P. mirabilis* to form biofilms on the cranberry-modified silicone surface is qualitatively studied over the course of 96 hours via confocal laser scanning microscopy and quantitatively studied using COMSTAT 2 image analysis and multiple analytical techniques. CDM-modified silicone demonstrated sustained release of approximately 30% of its

cranberry content into a lysogeny broth environment over the course of 96 hours. A positive correlation between cranberry concentration and storage modulus was observed, whereas ultimate tensile strength and elongation at break decreased with increasing concentrations of cranberry. Moreover, no change in the surface hydrophobicity of the CDM-modified silicone was detected via contact angle goniometry. The presence of cranberry in the silicon substrate was found to result in flattening of *P. mirabilis* biofilms, leading to significant increases in surface coverage and surface exposed to nutrients. Biovolume as determined by COMSTAT 2 and number of attached bacteria as determined by hemocytometry presented no difference between cranberry-modified silicone and control, whereas *P. mirabilis* viability was found to be higher on cranberry-modified silicone.

Résumé

Les infections urinaires attribuées à l'utilisation des cathéters sont le deuxième type le plus courant des infections nosocomiales en Amérique du Nord avec plus d'un million de cas à chaque année. Ce taux d'incidence élevé, en combinaison avec la dissémination d'uropathogènes résistants aux antibiotiques, a entraîné beaucoup d'intérêt dans le développement de mesures préventives au sein de la communauté de recherche. La consommation de *Vaccinium macrocarpon*, la canneberge de l'Amérique du Nord, est reliée à la prévention des infections bactériennes dans les voies urinaires depuis plus de 100 ans. Le Laboratoire de Biocolloïdes et Surfaces de l'Université McGill a démontré que les matériaux dérivés de canneberges (MDC) peuvent inhiber l'adhésion bactérienne aux surfaces, compromettre la motilité bactérienne, et influencer divers facteurs de virulence. Il est donc supposé que la canneberge et les matériaux dérivés de canneberges pourraient empêcher le développement des infections urinaires attribuées à l'utilisation des cathéters en perturbant les diverses étapes de la pathogénie de ce type d'infection. Dans ce document, nous faisons rapport sur la bioperformance d'une silicone biomédicale imprégnée de matériaux dérivés de canneberges contre la formation de biofilms d'un uropathogène cliniquement pertinent, *Proteus mirabilis*. En outre, la performance mécanique de ce matériau hybride est étudiée. Premièrement, la libération de matériaux dérivés de canneberges par la silicone est étudiée dans un milieu de culture LB pendant 96 heures utilisant une méthode spectrophotométrique. Deuxièmement, la résistance ultime à la traction, l'allongement à la rupture, le module de conservation, et l'angle de contact de ce matériau hybride sont décrits. Enfin, la capacité de

P.mirabilis de former des biofilms sur le matériau hybride pendant 96 heures est qualitativement étudiée via microscopie confocal à balayage laser (MCBL) et quantitativement étudiée utilisant le programme d'analyse d'image COMSTAT 2 ainsi que par multiples techniques analytiques. La libération d'environ 25% des MDCs par le matériau hybride dans un milieu de culture LB a été observée au cours de 96 heures. Une corrélation positive entre la concentration de MDC et le Module de Young a été observée, tandis que la résistance ultime à la fraction ainsi que l'allongement à la rupture ont diminué avec l'augmentation des concentrations de MDC. De plus, aucun changement de l'hydrophobicité de la surface du matériau hybride n'a été détecté. Une structure de biofilm plus plate a été observée sur la surface du matériau hybride en combinaison avec une plus grande couverture de surface et une plus grande surface de biofilm exposée au milieu de culture LB. Le biovolume calculé par COMSTAT 2 ainsi que le nombre de bactéries attachées sur la surface du silicone déduit par hémocytométrie ne présentaient aucune différence entre le matériau hybride et le matériau standard, tandis que la viabilité de *P.mirabilis* était supérieure sur le matériau hybride.

Acknowledgements

The completion of experimental work and writing of this thesis would not have been possible without the support and assistance of numerous people. I am especially thankful to my supervisor Professor Nathalie Tufenkji for the opportunity to work with her at the McGill Biocolloids and Surface Laboratory.

I would also like to acknowledge the support from numerous postdoctoral members of the Biocolloids and Surfaces Research Group who provided me technical advice and encouragement. Most particularly, I would like to thank Adam Olsson, Ché O'May, Zeinab Hosseini Doust, and Bahareh Asadishad for their ideas, opinions, and knowledge. Moreover, I would like to thank the rest of the McGill Biocolloids and Surface Laboratory for their moral support and lasting friendship.

Lastly, a special thanks to my parents, my brother, my sister, and Zoé Lacroix for their continuous support, understanding, and encouragement.

This project would not have been possible without financial support from Natural Sciences and Engineering Research Council of Canada, the Canada Research Chairs Program, and the Eugenie Ulmer Lamothe Fund in the Department of Chemical Engineering at McGill University.

Preface and Contribution of Authors

This thesis is submitted in compliance with the McGill University thesis preparation and submission guidelines and is formatted as a manuscript based thesis. Chapter 1 consists of a thesis introduction and summary of objectives. Chapter 2 contains a manuscript reporting the investigation of the biological and mechanical performance of cranberry-modified silicone materials for use in implantable medical devices. The manuscript will be submitted to *Colloids and Surfaces B* and authorship of the manuscript will be Louis Briggs, Showan Nazhat and Nathalie Tufenkji. Chapter 3 comprises the thesis conclusions as well as recommendations for future work.

The experimental work, data analysis, and writing of the manuscript were performed by Louis Briggs. Showan Nazhat provided some technical expertise. Nathalie Tufenkji provided guidance and expertise in a supervisory role throughout the project and in the manuscript revision.

Table of Contents

Abstract	i
Résumé.....	iii
Acknowledgements.....	v
Preface and Contribution of Authors.....	vi
Chapter 1: Thesis Introduction	1
1. Research incentive	1
2. Pathogenesis	3
3. <i>Proteus mirabilis</i> - model uropathogen	6
4. <i>Proteus mirabilis</i> HI4320 CAUTI biofilms	7
5. Silicone rubber in implantable medical devices	7
6. Review of current catheter technologies	8
7. Cranberry and Proanthocyanidins - Overview.....	9
8. Cranberry and CPACs – Proposed Mechanisms of Action	11
9. Thesis Objectives.....	13
Chapter 2: Investigating the biological and mechanical performance of cranberry-modified silicone materials for use in implantable medical devices	14
1. Introduction	14
2. Materials and Methods.....	18
2.1 Media & Bacterial Strain.....	18
2.2 Cranberry modified silicone preparation	18
2.3 Cranberry release from CDM-modified silicone.....	19
2.4 Biofilm growth on CDM-modified silicone	19
2.5 Biofilm imaging and image analysis.....	20
2.6 Biofilm disruption and quantification.....	21
2.7 Dynamic Mechanical Analysis (DMA)	21
2.8 Break and elongation force	22
2.9 Contact angle measurement	22
2.10 Statistical Analysis.....	22

3. Results and Discussion	23
3.1 Cranberry release from CDM-modified silicone	23
3.2 Mechanical Analysis of CDM-modified Silicone Substrate	24
3.3 Biofilm imaging and COMSTAT image analysis.....	27
3.4 Biofilm disruption, quantification, and viability	30
4. Acknowledgements.....	33
Chapter 3: Conclusion and Suggested Future Work	34
References	36

Table of Figures

Figure 1: Structure of a proanthocyanidin molecule formed by one A-type linkage and two B-type linkages	10
Figure 2: Release profiles for varying concentrations of CDM into LB broth from LSR30 biomedical grade silicone. Error bars represent the standard deviation (SD) of triplicate samples. A greater relative % of CDM from 5% coupons is released over the 96 hour time period as compared to the 10% coupons.	24
Figure 3: Light microscopy image of a 5% CDM-modified silicone coupon at 200x magnification. CDM aggregates are observed throughout the material's thickness.....	24
Figure 4: Dynamic mechanical analysis performed on 0, 5 and 10% CDM-modified silicone coupons. Storage modulus is shown to increase with increasing CDM concentration and with increasing frequency, however not significantly.	26
Figure 5: Sample CLSM images of <i>Proteus mirabilis</i> biofilms grown on control and CDM-modified silicone over 96 h. 0%, 5%, and 10% CDM coupons are shown in images a, b, and c, respectively.	27
Figure 6: Computational results from COMSTAT 2 image analysis and area fraction measurements by ImageJ. No significant differences in biovolume and average thickness are observed whereas significant differences are observed in regards to area fraction (One-way ANOVA, [F(2,51)=17.68, p<0.05]) and area exposed to media (One-way ANOVA, [F(2,75)=4.56, p<0.05]). Comparison of CDM coupons to control coupons was performed by <i>post hoc</i> t-tests where significance (p<0.0167, Bonferroni corrected α) is indicated by (*). Upper and lower box limits represent the top and bottom quartiles, center lines represent the median, (▪) represent the average, whiskers represent 5 th and 95 th percentiles, and (°) represent any outliers.	28
Figure 7: Bacteria/mL and CFU/mL determined via hemocytometry and the Miles and Mistra method, respectively. No significant changes in bacteria count via hemocytometry is observed, however a significant increase (p<0.05) in colony forming units is observed on CDM-modified coupons.....	31

Table of Tables

Table 1: Virulence factors of <i>Proteus mirabilis</i> with potential role in biofilm formation. Adapted from Jacobsen and Shirtliff [23].....	7
Table 2: Elongation at break, ultimate tensile strength, and contact angle measurements reported for 0, 5 and 10% CDM-modified coupons. Using a one way ANOVA, no significant change in elongation at break, ultimate tensile strength, and contact angle was found between 0, 5, and 10% CDM modified coupons with $p>0.05$ in all cases.	26

Chapter 1: Thesis Introduction

1. Research incentive

Catheter associated urinary tract infections (CAUTIs) have become the most common medical device associated infections in North-American hospitals, with 15 to 25% of all hospitalized patients receiving urinary catheters during their hospital stay [1]. CAUTI daily incidence rates of 3-7% have been reported for patients with indwelling catheters, leading to 30 day incidence rates approaching 100% [2, 3]. Over half a million cases of urinary tract infection were reported in the United States alone in 2007, with 80% of infections caused by indwelling catheters - CAUTIs currently represent 26% of all healthcare-associated infections [4].

High infection rates coupled with high direct medical costs drive research in the prevention of CAUTIs. The average cost of an episode of CAUTI is US\$900 (adjusted for inflation based on 2000 data), however catheter-related bacteremia can incur hospital costs exceeding US\$3,700 (adjusted for inflation based on 2000 data) [5]. These direct hospital costs are primarily made up of laboratory diagnostics and pharmaceutical costs which now incur a yearly US expenditure of US\$500 000 000 [6].

The development of CAUTIs arises from both the extraluminal acquisition of endogenous organisms and the intraluminal acquisition of exogenous organisms [6]. It is a variety of bacteria types and strains that are ultimately responsible for the infections. The most common uropathogens are Gram negative lactose fermenting rod shaped coliforms: *Escherichia coli*, *Klebsiella spp.*, *Serratia spp.*, *Citrobacter spp.*, and *Enterobacter spp.* Non-coliform

uropathogens of this form also exist, with the most common being *Proteus spp.* and *Pseudomonas aeruginosa*. Gram positive uropathogens include *Enterococcus spp.*, *Staphylococcus aureus*, coagulase negative staphylococci, and yeasts such as *Candida spp* [7]. Overall, the most common uropathogens associated with CAUTI as reported by the Center for Disease Control and Prevention are *Escherichia coli* (21.4%), *Candida spp.* (21.0%), *Enterococcus spp.* (14.9%), *Pseudomonas aeruginosa* (10.0%), *Klebsiella pneumoniae*(7.7%), and *Enterobacter spp.* (4.1%) [8].

The dissemination of antibiotic resistant uropathogens in both hospitals and communities has created much interest in the development of preventative measures within the research community. As demonstrated by Rajesh, Mathavi [9], the majority of common uropathogens now present resistance to antibiotic standards for UTI treatment. Important examples include the drugs Ciprofloxacin and Cotrimoxazole (commonly prescribed antibiotics for UTI) to which nearly all uropathogenic species now demonstrate resistance [9]. It is therefore understandable that the new technologies and methods under development are aimed at reducing the use of antibiotics. Examples of these new technologies include portable ultrasound devices to assess catheterization requirements, antiseptic- or antimicrobial-impregnated catheters such as silver-alloy coated catheters, and guidelines/algorithms for improved perioperative catheter management [10]. However, in order to best understand the viability of these new methods, it is important to understand the pathogenesis of urinary tract infections.

2. Pathogenesis

There are three principal routes of entry to the bladder that are associated with the use of urinary catheters: bacteria colonizing the distal urethra are pushed towards the bladder during catheter insertion, bacteria colonizing the distal urethra travel along the outside of the catheter towards the bladder using several forms of motility, and bacteria contaminating catheter junctions, collection bag, or sampling ports climb in the inside of the catheter towards the bladder using several forms of motility. A study by Tambyah, Halvorson [11] reported that 18% of infections were caused by unsterile insertion, 48% by extraluminal climbing, and 34% by intraluminal climbing [11]. These results demonstrate that motility is one of the first steps in the colonization of the bladder by uropathogens and could play a crucial role in the onset of CAUTI. Five types of bacterial motility can be described to explain the movement of uropathogens up the urethra towards the bladder: swarming, swimming, twitching, gliding, and sliding.

Swarming motility appears to be limited to specific species within three families of the Bacteria domain. These three families, Firmicutes, Alphaproteobacteria and Gammaproteobacteria, include the swarming species *Escherichia coli*, *Proteus mirabilis*, and *Pseudomonas aeruginosa* which are all commonly known uropathogens [12]. Swarming consists of the rapid and aggregated movement of bacteria along a surface using powered rotating flagella [12]. Because of its rapidity, it is thought to be one of the principal motifs for movement along the catheter surface. Swarming differs from bacterial swimming which consists of the movement of single bacteria throughout a liquid medium. Swimming motility would allow uropathogens to travel within a urine-filled catheter, or within the bladder itself [13]. Twitching motility comprises

movement along a surface, but instead of using rotating flagella, twitching motility uses type IV pili that extend and retract to cause twitch-like movements. It can take place on either organic or inorganic surfaces and is suspected to be a mode of transport in environments with low water content [14]. Gliding is another form of powered bacterial movement that occurs on surfaces, however it does not use flagella or pili. Instead, the gliding motion originates from movement along the long axis of the cell due to focal adhesion complexes that bind to the surface substrate [15]. Finally, there is sliding which is the only form of non-powered motility. It is highly dependent on the presence of surfactants on the substrate surface that can reduce surface tension and ultimately allow the cells to be pushed away from the origin due to pressure from cell growth [13].

Once in the bladder, uropathogens are in the presence of uroepithelial cells, stagnant urine below the inflatable portion of the catheter, and the catheter material itself [16]. Although the presence of stagnant urine below the inflatable balloon of the catheter has not been shown to enhance the development of CAUTI, it prevents the drainage of bacteria from the bladder. Adhesion of uropathogens to uroepithelial cells is well documented, and incorporates the use of specific adhesins on the surface of fimbriae and flagella. Adhesion to catheter materials has proven more complex, varying with both material and bacteria type [16]. The adhesion process is important as it leads to the formation of biofilms, which are the primary contributor to catheter encrustation, blockage, resistance to antibiotic treatment, and repeated occurrence of CAUTI.

Biofilms consist of communities of cells that have adhered to a surface and that have excreted a polysaccharide matrix. The development of these films is highly structured and comprises multiple steps: adsorption of organic polymers to the surface, adhesion of bacteria to cell surface using adsorbed molecules, formation of microcolonies and secretion of extracellular polysaccharide matrix, and detachment for film expansion [17]. Once the biofilm has been established on the catheter within the bladder, encrustation is often observed. Observation of this phenomenon is however limited to cases in which biofilms form in a urine environment. Although considered a variable fluid [18], urine from a healthy adult is usually 95% water, with the remaining 5% comprising organic molecules (urea, creatinine, uric acid, hormones, mucins, enzymes, etc) and ions (sodium, potassium, magnesium, calcium, ammonium, sulphates, phosphates, etc). Urine pH varies widely between people with values between pH 4.5-8 with an average of pH 6. These properties make urine an excellent medium for bacterial growth. Catheter encrustation in this urine environment is caused by the urease produced by the uropathogens which breaks down urea to ammonia which in turn increases the pH of the urine and precipitates potassium and magnesium salt crystals. These crystals then adhere to the biofilm surface where they are protected by the extracellular polysaccharide matrix and can withstand changes in pH [19]. Studies of *Proteus mirabilis*, *Proteus vulgaris* and *Providencia rettgeri* were able to raise the urinary pH to above 8.3 and produce catheter-blocking crystalline biofilms within 40 h. Further studies by McLean, Lawrence [20] have shown that this biofilm protection effect allows crystals to remain intact in flow conditions of pH 5.8 urine up to 200 mL/hour (normal human urine output is 50 mL/h) whereas free floating crystals dissolved within 10 minutes of exposure to 4 mL/h flow [20].

Additional virulence factors are expressed by uropathogens once they have colonized the bladder and urethra. These virulence factors include hemolysis, proteolysis, the capacity to cause mannose-resistant hemagglutination (MRHA), and serum resistance [21]. Of primary importance are hemolysis and MRHA which are linked to renal disease and pyelonephritis, respectively. α -hemolysin causes strong inflammatory responses and leads to the secretion of chemotaxins whereas the capacity to cause MRHA is due to various fimbriae that adhere to fibronectin on uroepithelial cells [22].

3. *Proteus mirabilis* - model uropathogen

Proteus mirabilis, the most studied species of the *Proteus* genus and member of the Enterobacteriaceae family, is a Gram negative facultatively anaerobic rod shaped bacteria known for its swarming ability and prevalence as a causative agent for a wide variety of nosocomial infections [23]. Infections of the respiratory tract, eye, ear, nose, skin, burns, throat, wounds, and especially the urinary tract of individuals with structural/functional abnormalities such as the presence of a urinary catheter have been reported [24]. *P.mirabilis* is armed with a variety of virulence factors which contribute to its pathogenicity. These include multiple fimbriae, flagellar motility, immunoavoidance factors (antigenic variation, capsules, IgA proteases, lipopolysaccharides, ZapA), host damaging factors (proteases, ureases, hemolysins), struvite and hydroxyapatite crystal formation, iron acquisition protein homologs, and the ability to form biofilms [24]. The combination of these virulence factors make *P.mirabilis* an aggressive agent in the onset of CAUTI as well as one of the most difficult to treat. *P.mirabilis* is therefore proposed as an important model pathogen in the study of CAUTI.

4. *Proteus mirabilis* HI4320 CAUTI biofilms

P. mirabilis has been shown to form biofilms on a variety of non-living materials including polystyrene, glass, latex, and silicone [20]. The structure of these biofilms in pooled human urine as well as Luria Bertani broth on glass substrate has been studied [25, 26] and shown to have a typical mushroom-like structure accompanied by the formation of water and nutrient channels throughout. A variety of virulence factors have been associated with the formation of these biofilm structures, and were summarized by Jacobsen and Shirtliff [23].

Table 1: Virulence factors of *Proteus mirabilis* with potential role in biofilm formation. Adapted from Jacobsen and Shirtliff [23]

Virulence Factors	Proposed Role
Mannose-resistant <i>Proteus</i> -like (MR/P) fimbriae	Adhesion, mutants defective in biofilm formation
UDP-glucuronic acid decarboxylase Pmrl	LPS modification, mutants defective in biofilm formation
Inne-core LPS biosynthetic WaaE	Inner-core LPS biosynthetic protein, mutants decrease in biofilm formation
Pst transporter	High-affinity phosphate transporter, mutants defective in biofilm formation
RsbA	Membrane sensor of a two component system that enhance EPS production in the presence of certain fats
CIS-2-decenoic acid	Homolog of <i>Pseudomonas</i> cell communication factor, role in dispersal and inhibition of biofilm development
RsmA	RNA binding protein, possible regulation of biofilm formation
Urease	Nickel metalloenzyme, local increase in pH to facilitate crystal formation, Mutants attenuated in CBA mouse model
Capsule	Aggregate precipitating components into stones

5. Silicone rubber in implantable medical devices

Silicone, a type of synthetic polymer with a backbone made of repeating silicon to oxygen bonds, has found widespread use in healthcare due to its biocompatibility and biodurability [27]. In more detail, silicones present ideal hydrophobicity, low surface tension, gas permeability, and high chemical and thermal stability. These properties can be associated with

the high binding energy of siloxane bonds and the low intermolecular forces between silicone molecules [28]. It is these properties that have made silicone rubbers the most thoroughly tested and used biomaterials for medical applications. For instance, urinary catheters have now been manufactured of silicone or silicone coated substrates for over 60 years [28]. Despite these properties, there are certain limitations to consider when using silicone rubber in medical applications. Mainly, silicone rubbers exhibit poor tear strength and poor resistance to fatigue, which are important factors in implant design [29].

6. Review of current catheter technologies

Antimicrobial-impregnated catheters containing a variety of broad-spectrum antibiotics such as nitrofurazone, minocycline, and rifampin have been studied for the prevention of bacterial CAUTIs. These catheter designs have proven highly effective in reducing the number and severity of CAUTIs, however the issue of bacterial resistance has not been resolved [30].

A more recent trend in urinary catheter design has involved coating or embedding catheters with silver alloys, silver hydrogels, silver nanoparticles, silver electrodes, and silver oxide. The ability of silver to kill bacteria is well documented in the literature and is caused by the formation of silver ions in solution which disrupt bacterial membranes and subsequently kill the bacteria. Despite positive *in vitro* studies, conflicting clinical trials question the use and efficacy of silver-based catheters. A randomized clinical trial of 1309 patients failed to demonstrate the effectiveness of silver oxide coated silicone catheters [31], a study at the University of Massachusetts Medical Center demonstrated a non-significant reduction in CAUTIs with use of

silver-hydrogel catheters [32], and the use of silver electrodes prevented biofilm development of *P. mirabilis* *in vitro*, however the silver electrodes disintegrated after only 150 h of use [33].

Even newer approaches to biofilm prevention on urinary catheters comprise the utilization of biofilm inhibitor molecules, hydrophilic coatings, nutrient scavenging materials, lytic bacteriophage coatings, and various forms of mechanical disruption [24]. Biofilm inhibitor molecules often encompass compounds that inhibit quorum sensing signal molecules as these compounds have been shown to be important to bacteria coordination and subsequent biofilm formation [34]. Furocoumarins from grapefruit juice, for example, were shown to inhibit autoinducer signaling within bacteria populations, effectively inhibiting biofilm formation [35]. Hydrophilic coatings such as those on the LoFric Foley catheters have demonstrated less hematuria and a decrease in the incidence of urinary tract infections [36]. Nutrient scavenging materials also show promise for biofilm prevention by depriving bacteria of nutrients key to biofilm formation. The gene for iron acquisition in *P. mirabilis*, for example, has been identified as a key component for infection of the urinary tract [37]. Lastly, several forms of mechanical disruption techniques have been developed. Examples include the use of acoustic energy, which did not disrupt biofilm structures of *Pseudomonas aeruginosa* but increased antibiotic uptake of the biofilm, and disruption via applied strain as recently demonstrated by Levering, Wang [38] who were able to demonstrate release of mature *P. mirabilis* biofilms from strained surfaces [38].

7. Cranberry and Proanthocyanidins - Overview

Previous research conducted at the McGill Biocolloids and Surfaces Laboratory has shown that cranberry derived proanthocyanidins (CPACs) can inhibit bacterial adherence to surfaces and

also impair bacterial motility and influence various bacterial virulence functions [39-41]. It is therefore hypothesized that cranberries and cranberry derived materials could prevent the development of CAUTIs through the inhibition of pathogenesis. CPACs are polyphenolic compounds produced by the cranberry as a protective agent against environmental hazards and microbial attack. They are built of two different flavonoid subunits, catechin and epicatechin which are attached via A-type and B-type interflavanyl linkages; it is the uncommon A-type linkages that are believed to impart unique anti-adhesion properties to the CPAC compounds [42]. A degree of polymerization of 4 or 5 subunits has been demonstrated as the most effective for the inhibition of uropathogen adhesion to uroepithelial cells [42, 43]. Figure 1 depicts the structure of a proanthocyanidin made up of 3 subunits bound by two B-type linkages and one A-type linkage [42, 43]. The A-type linkage can be identified as the combination of a carbon-carbon single bond and an ether carbon-oxygen bond.

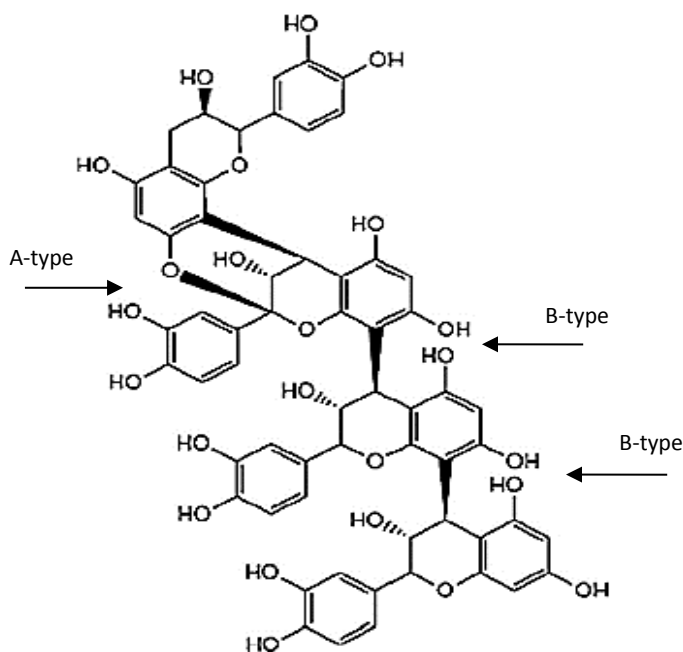


Figure 1: Structure of a proanthocyanidin molecule formed by one A-type linkage and two B-type linkages

8. Cranberry and CPACs – Proposed Mechanisms of Action

Three principal mechanisms of action have been proposed to explain the role of cranberry and CPACs in the prevention of CAUTI:

- 1- Impairment of bacterial adhesion to cells and materials: Cranberry has been shown to alter cell surface properties [44, 45], alter bacterial morphology and shape [46], interfere with P-type fimbriae [47], bind to bacterial cell membrane LPS [48], and cause cytoskeleton rearrangement of host cells reducing formation of focal adhesion points or pedestals used for bacteria-cell interaction [49]. Further, cranberry and cranberry derived materials have been shown to inhibit adhesion of bacteria to human host cells [42, 50, 51]. In regards to adhesion to biomaterials, cranberry derived materials have demonstrated the ability to reduce attachment strength and non-specific binding of bacteria to a variety of biomaterials [44, 52, 53].
- 2- Impairment of bacterial motility: CPACs were shown to have little to no effect on the swimming and twitching motilities of *Pseudomonas aeruginosa*, however a significant impairment of swarming motility was discovered [40]. In *E.coli*, cranberry was linked to the downregulation of the flagellin gene (*fliC*) which precludes the synthesis of flagella [40]. Further, swimming and swarming motilities of *Proteus mirabilis* and swarmer-cell differentiation were shown to be inhibited by cranberry [54].
- 3- Impairment of iron uptake: CPACs was demonstrated to induce a state of iron limitation on uropathogenic *E. coli* and a reduction in urease expression in *P.mirabilis* [54, 55].

The aforementioned promising effects of cranberry and CPAC primarily comprise adhesion, motility, and iron uptake. The effect of cranberry and cranberry derived materials on biofilm formation is however not completely understood and recent research has shown mixed results. Several studies have reported no effect or an enhancing effect by cranberry on biofilm formation [39, 56], whereas other studies have demonstrated inhibitory effects [57-60]. Therefore, to better understand the potential role of cranberry derived materials in the prevention of CAUTI biofilms, it is proposed to study the bioactivity of cranberry materials embedded in biomedical grade silicone against biofilm formation and to mechanically characterize this material for potential catheter manufacturing.

9. Thesis Objectives

The primary objectives of this thesis were to impregnate biomedical grade silicone with cranberry derived materials to assess the hybrid materials' bioperformance against *Proteus mirabilis* biofilms and to characterize the change in the materials' mechanical performance. The research was performed to test the hypothesis that the presence of cranberry derived materials in biomedical grade silicone would interfere with *Proteus mirabilis* biofilm formation on the silicone surface. Further, it was hypothesized that the addition of cranberry derived materials to biomedical grade silicone would alter the mechanical properties of the silicone which are important to urinary catheter manufacturing. Thesis objectives are summarized as:

1. Qualitatively and quantitatively characterize *Proteus mirabilis* biofilms on CDM-modified silicone using confocal laser scanning microscopy and COMSTAT image analysis
2. Qualitatively and quantitatively characterize *Proteus mirabilis* biofilms on CDM-modified silicone via disruptive techniques
3. Characterize mechanical properties of CDM-modified silicone via dynamic mechanical analysis, elongation and force at break, and surface contact angle

Chapter 2: Investigating the biological and mechanical performance of cranberry-modified silicone materials for use in implantable medical devices

1. Introduction

Catheter associated urinary tract infections (CAUTIs) are the second most common hospital acquired infections in North America [61], with daily incidence rates reaching 7% for the 15-25% of all hospitalized patients who require the use of an indwelling urinary catheter during their hospital stay. CAUTIs lead to many medical complications, including cystitis, pyelonephritis, bacteremia, prostatitis, epididymitis, orchitis, endocarditis, vertebra osteomyelitis, septic arthritis, endophthalmitis, and meningitis, as reported by the Centre for Disease Control and Prevention [62]. These complications not only add to the discomfort of patients, but extend hospital stays, lead to higher mortality rates, and impose a significant financial burden on the health-care system.

The pathogenesis of CAUTIs can be summarized by a series of events. The first comprises three potential points of entry coupled with multiple forms of bacterial motility. Bacteria colonizing the distal urethra can be pushed towards the bladder during catheter insertion, bacteria colonizing the distal urethra can travel along the outside of the catheter towards the bladder, and bacteria contaminating catheter junctions, the collection bag, or sampling ports can reach the bladder via the inside of the catheter using several forms of motility. Next, bacteria colonise the bladder using urine as their nutrient source and initiate attachment to host cells and the catheter surface using an assortment of adhesins. This process is facilitated by the deposition of

a conditioning film made up of proteins, electrolytes, and other organic molecules that neutralize any engineered anti-adhesive properties of the catheter surface [63]. Now attached to the catheter or uroepithelium, the bacteria begin a phenotypical change where they produce exopolysaccharides that envelop and protect the bacteria. This process combined with continued bacterial growth leads to the formation of three dimensional cooperative bacterial communities called biofilms. Lastly, uropathogens further adapt to the host environment using a series of virulence factors. Degradative excretions break down urine components as well as host tissues which in turn release digestible nutrients for bacteria uptake. Examples include the enzyme urease for breakdown of urea, ferric and ferrous iron transport systems for iron uptake, and hemolysins. Bacteria must also fight host immune evasion, and do so via a number of mechanisms which include the production of capsules, immunoglobulin A, proteases, and lipopolysaccharides [64] .

From the pathogenesis of infection, it can be noted that biofilm formation is the central character in the story of CAUTI [65]. Biofilms provide survival advantage to the bacteria in multiple ways: resistance to shear forces from urine flow, resistance to invasion by host immune cells, and resistance to antimicrobial agents. The highly structured and polymerized nature of the biofilm is what confers the resistance to shear forces (catheter blockage by biofilms can also significantly reduce urine flow), whereas biofilms have been shown to induce a weaker leukocyte response as compared to their planktonic counterparts. Further, bacteria in biofilms have been shown to have slower growth rates which reduces uptake of antibiotics, and facilitated transfer of antimicrobial resistance genes that confer antibiotic resistance [66].

Research and development in the area of biofilm-resistant catheters has led to a variety of modern catheter designs. Examples of these designs include antimicrobial-impregnated catheters containing a variety of broad-spectrum antibiotics, coating or embedding catheters with silver alloys, silver hydrogels, silver nanoparticles, silver electrodes, and silver oxide, and more recent designs comprising the utilization of biofilm inhibitor molecules, hydrophilic coatings, nutrient scavenging materials, lytic bacteriophage coatings, and various forms of mechanical disruption [24]. Despite these advances, there is still no comprehensive solution to prevent formation of CAUTI biofilms due to the development of antibiotic resistance, surface deactivation by conditioning films, and the long periods of time for which these catheters must remain active. Continued research in catheter material design is therefore warranted.

Consumption of the North American cranberry, *Vaccinium macrocarpon*, has been linked with the prevention of urinary tract infection for over 100 years. The mechanism by which cranberry prevents urinary tract infections is not entirely understood, however recent studies have demonstrated cranberry's ability to impair bacterial adhesion, motility, and nutrient uptake systems. Impairment of bacterial adhesion to cells and materials is accomplished via alteration of cell surface properties [44, 45] alteration of bacterial morphology and shape [46], interference with P-type fimbriae [47], binding to bacterial cell membrane LPS which blocks LPS-TLR4/MD2 interactions [48], and cytoskeleton, rearrangement of host cells reducing formation of focal adhesion points or pedestals used for bacteria-cell interaction [49]. This impairment of adhesion is demonstrated by cranberry's ability to reduce adhesion of bacteria to epithelial cell receptors [42], cultured bladder cells [50], uroepithelial cells [51], and biomaterials such as glass [53], silicone rubber [44], poly(vinyl chloride), and

polytetrafluoroethylene [52]. In regards to motility, cranberry has been shown to significantly impair the swarming motility of *Pseudomonas aeruginosa* [39] and was linked to the downregulation of the flagellin gene (*fliC*) which precludes the synthesis of flagella in *E. coli* [41]. Further, swimming and swarming motilities of *Proteus mirabilis* and swarmer-cell differentiation were inhibited by cranberry [54]. In regards to nutrient uptake, a state of iron limitation in uropathogenic *Escherichia coli* CFT073 was induced by cranberry-derived proanthocyanidins and urease expression was also shown to be inhibited by cranberry [54, 55]. Based on the important roles of adhesion, motility, and nutrient uptake in biofilm formation, it is suspected that cranberry could play an important role in the prevention of CAUTI biofilms.

Previous research by the McGill Biocolloids and Surfaces Laboratory demonstrated the incorporation of cranberry derived materials (CDMs) into industrial and biomedical grade silicone [67]. Chan et al reported the release of bioactive cranberry material into an aqueous environment and subsequent decrease in the production of flagellin in both *E. coli* and *P.mirabilis* leading to impaired motility on the surface of the cranberry-modified silicone [67]. The effect of cranberry release from silicone on biofilm formation is however not yet understood. In this study, the ability of *Proteus mirabilis* H14320 to form biofilms on CDM-modified silicone is examined via confocal laser scanning microscopy and multiple analytical techniques. Further, storage modulus, ultimate tensile strength, elongation at break, and contact angle are reported to assess the mechanical performance of the silicone-cranberry hybrid material.

2. Materials and Methods

2.1 Media & Bacterial Strain

Proteus mirabilis H14320 isolated from the urine of an elderly long term-catheterized woman is the uropathogen used in this study. This organism was previously described by Mobley and Warren [68] , and sequenced and annotated by Pearson et al. [69].

Proteus mirabilis was routinely grown in Luria-Bertani (LB) broth (10 g/L tryptone, 5 g/L yeast extract, and 5 g/L NaCl) at 37°C with rotary shaking at 150 RPM after being aseptically inoculated from culture grown from -80°C stock streaked onto low-swarm (LSW⁻) agar plates (10 g/L tryptone, 5 g/L yeast extract, 5mL/L glycerol, 0.4 g NaCl, and 20 g/L agar) supplemented with 1 mL/L of 1M MgSO₄, 10 mL/L of 20% glycerol, and 1 mL/L 1% nicotinic acid post-autoclave sterilization [70, 71]. Phosphate buffered saline (PBS) solution was prepared by dissolving PBS tablets (Sigma-Aldrich) in deionized water and was autoclaved for sterilization. All media were prepared using deionized water (DI; Milli-Q).

Cranberry powder (CP) from dehydrated whole crushed cranberries (Atoka Cranberries, Quebec, Canada) was used as the CDM of interest in this study.

2.2 Cranberry modified silicone preparation

LSR30 Implant Grade Silicone and Curing Agent (Applied Silicone, California) was used as a base polymer for cranberry-modified silicone preparation. The two part silicone mixture comprises a dimethyl silicone elastomer designed to be mixed at 10 parts base to 1 part crosslinker. Cranberry powder was incorporated into the two part silicone mixture at concentrations of 0, 5

and 10 weight percent as previously described by Chan et al. [67]. After thorough mixing, the mixture was desiccated to remove excess hydrogen gas formed by polymerization and any other gases incorporated by mixing. The mixture was then poured into stainless-steel moulds of 1 mm thickness and cured at room temperature under 5 kN of pressure for 48 hours. The resulting silicone sheets were then stamped into circular coupons of 0.5" diameter for biofilm assays or cut into 50mm×5mm strips for mechanical testing. All silicone samples were sterilized by UV irradiation for 30 minutes prior to use.

2.3 Cranberry release from CDM-modified silicone

CDM release from silicone coupons was measured via spectrophotometry. Coupons were submerged in 750 μ L LB broth in separate wells of a 24-well plate (polystyrene, Corning Life Sciences). The plate was subsequently incubated at 37°C with rotary shaking at 150 RPM. Periodically, the OD₂₈₀ of the LB broth supernatant was measured (Biomate 3, Thermo Scientific) with purpose of determining the dissolved concentration of CDM from standard curves. A strong linearity between CDM concentration and absorbance at 280 nm was determined with an R^2 value of 0.9861. 280 nm was chosen as it is the peak absorbance wavelength for CPAC [30]. Controls were performed with unmodified LSR30 implant grade silicone to assure no interfering compounds were released from the silicone material.

2.4 Biofilm growth on CDM-modified silicone

Proteus mirabilis biofilms were grown following preparation of the CDM-modified silicone substrates. Coupons measuring 0.5" in diameter and 1 mm in thickness were pressed to the

bottom of each well of a 24-well plate (Polystyrene, Corning Life Sciences). Wells were subsequently filled with 750 μ L of 100 \times diluted overnight culture of *Proteus mirabilis* in LB broth. 24-well plates were then incubated at 37°C with rotary shaking at 150 RPM for 96 hours. Prior to analysis, samples were gently rinsed 3 times with 750 μ L PBS.

2.5 Biofilm imaging and image analysis

Confocal laser scanning microscopy was performed on biofilm samples for qualitative and quantitative analysis of *Proteus mirabilis* biofilms on CDM-modified silicone substrate. Coupons were stained using SYTO-9 green fluorescent nucleic acid stain (BacLight LIVE/DEAD, Molecular Probes) following the guidelines provided by the manufacturer. Biofilms were not stained with the propidium iodide component of the staining kit due to the excitation wavelength overlap with that of CPAC (280 nm). Following staining, samples were imaged in triplicate using a Zeiss LSM 510 META equipped with argon laser (458 and 488 nm) set to one channel (CH: BP 505-530). A total of 9 z-stack images were taken on each sample, using a grid of fixed X-Y positions to ensure fair image sampling. Clean, non-wetted silicone samples as well as clean 96-hour wetted silicone samples were used as negative controls. No fluorescent signals were obtained from these controls (images not shown). COMSTAT 2 [72-74] was used for quantitative assessments of biovolume, surface area exposed to nutrients, and average biofilm thickness. Automatic thresholding using Otsu's method was selected for all images. Further, maximum intensity projections of all images were made using ImageJ, converted to binary, and measured for surface area fraction.

2.6 Biofilm disruption and quantification

96 hour biofilm-coated CDM-modified silicone coupons were gently rinsed 3 times with PBS and transferred to a clean 24-well plate. Wells were subsequently filled with 500 μ L of 0.25% trypsin (Gibco Trypsin-EDTA, Life Technologies) and left at room temperature for 10 min. A cell scraper was then used to mechanically disrupt the biofilms, followed by the addition of human serum to attenuate the enzyme activity and retain cell viability. The 24-well plate was then sonicated for 3 min to ensure complete biofilm disconnect from the silicone substrate. Coupons were then stained with SYTO-9 and imaged under CLSM to visually inspect for biofilm removal. Images confirming this disruption technique showed insignificant fluorescent signals (images not shown). The resulting cell suspensions were then individually mounted on a hemocytometer for enumeration under phase-contrast microscopy (IX-71, Olympus) at a magnification of 200 \times . Also, the collected cells were re-suspended and serially-diluted in PBS to perform surface viable counts using the Miles and Misra method [31]. Counts were performed on LSW agar plates after 18 hour incubation at 37°C in a humidified incubator.

2.7 Dynamic Mechanical Analysis (DMA)

Unmodified and CDM-modified silicone substrate was investigated by dynamic mechanical analysis. A sinusoidal varying tensile force was applied to silicone strips of dimension 5mm \times 50mm \times 1mm using an Electroforce Biodynamic test instrument equipped with a Bose 20N load sensor (Biodynamic System 5170; Bose Corp., Eden Prairie, MN). Vertical, uniaxial load at frequencies from 0.1 Hz to 5 Hz was applied with the purpose of determining the storage modulus. All measurements were repeated at least 3 times.

2.8 Break and elongation force

The ultimate tensile strength, break-force, and elongation at break of unmodified and CDM-modified silicone strips of dimension 5mm×50mm×1mm were determined using a EZ-test universal testing machine (Shimadzu Corporation), equipped with a 500N load sensor. A crosshead speed of 500 mm/min at a grip distance of 2 cm was used. All measurements were repeated at least 3 times.

2.9 Contact angle measurement

Contact angle goniometry was used to measure the degree of hydrophobicity of the CDM-modified silicone substrate. Samples were rinsed 3 times in DI and dried in a stream of high purity nitrogen gas. Triplicate equilibrium contact angle measurements were performed on each sample using an OCA-30 goniometer (Future Digital Scientific Corp., NJ,USA) on sessile drops (3 μ L) by measuring the tangent to the drop (averaging both right and left side of the drop) at its intersection with the surface.

2.10 Statistical Analysis

Where indicated, statistical significance between the effects of CDM-modified silicone and non-treated controls was determined using one-way ANOVA and *post hoc* t-tests with Bonferroni correction.

3. Results and Discussion

3.1 Cranberry release from CDM-modified silicone

It is of interest to confirm the concentration of cranberry present in the aqueous environment surrounding the CDM-modified coupons during biofilm growth. The release of bioactive CDMs from CDM-modified silicone was previously reported by Chan et al. [67] in a DI environment over a 24 hour period. Herein, we extended the study to a 96 hour period and performed the analysis in LB broth, the study medium of interest, to assess any effects on CDM release by the presence of peptides, vitamins, trace elements, and minerals. Preliminary experiments conducted using Brook's artificial urine medium [43] revealed considerable precipitation of the medium at 37 °C, thereby hindering the reproducibility of the experimental work. Therefore, LB medium was selected as the medium of interest. Sustained release of CDMs was observed with no significant differences between DI [67] and LB broth, indicating that diffusion is not affected by components of the Luria-Bertani broth. At the end of the 96 hour period, the 5% CDM coupons showed a higher relative total release as compared to the 10% CDM coupons. It was therefore inferred that the release rate of CDMs is disproportional to the CDM concentration gradient in the aqueous environment and that the CDM concentration within the silicone polymer lattice affects the diffusion process. The release of CDMs from the coupons is suspected to be caused by the sorption of water into the polymer matrix due to the hydrophilic nature of the CDM material. Higher concentrations of CDM may lead to larger CDM aggregates within the bulk material, effectively reducing the surface area for water sorption and slowing

the relative release rate. After a 96 hour period, CDM-modified coupons had released no more than a third of their CDM content, indicating potential for longer term release.

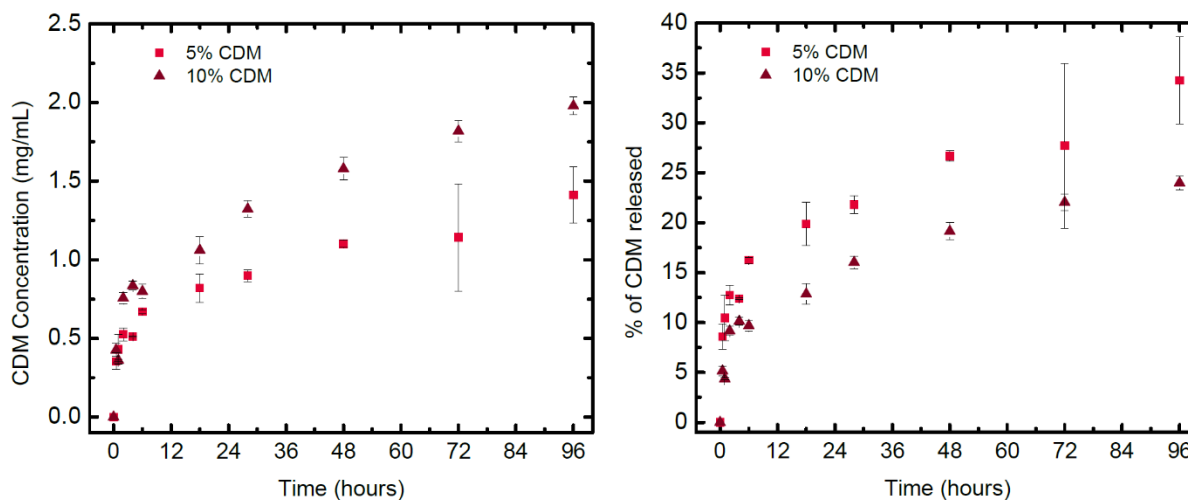


Figure 2: Release profiles for varying concentrations of CDM into LB broth from LSR30 biomedical grade silicone. Error bars represent the standard deviation (SD) of triplicate samples. A greater relative % of CDM from 5% coupons is released over the 96 hour time period as compared to the 10% coupons.

3.2 Mechanical Analysis of CDM-modified Silicone Substrate

Polymer integrity is important to the manufacturing process of urinary catheters. Previous studies pertaining to the incorporation of compounds into the silicone polymer matrix with subsequent release have shown changes to ultimate tensile strength, elastic modulus, elongation at break, and contact angle [75-77]. Understanding how polymer properties change during drug release

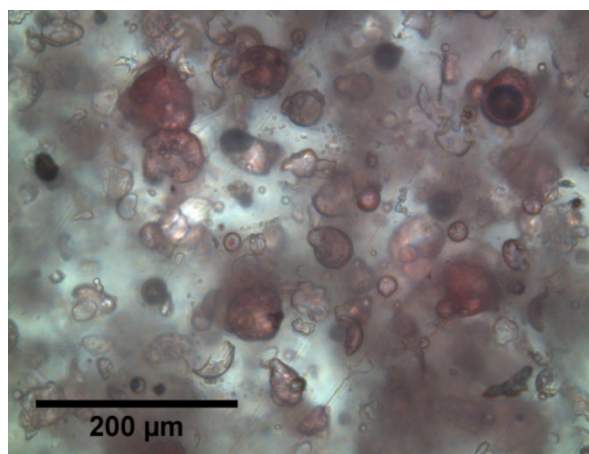


Figure 3: Light microscopy image of a 5% CDM-modified silicone coupon at 200x magnification. CDM aggregates are observed throughout the material's thickness.

is also important as catheters must retain their mechanical integrity throughout use. Further, certain mechanical properties also contribute to the material's ability to resist microbial invasion. For example, surface contact angle was demonstrated to affect biofilm initiation, whereby more hydrophilic surfaces were more resistant to biofilm initiation than hydrophobic surfaces [78]. In the same study, the smoothest surfaces showed the least biofilm initiation and easiest removal by standard shear stresses [78]. Moreover, a study of substrate mechanical stiffness showed that the adhesion of *S. epidermis* and *E. coli* correlated positively with the stiffness of a polymeric substrate, independent of roughness, interaction energy, and charge density [79]. These results indicate the possibility of mechanoselective adhesion mechanisms and suggest that mechanical stiffness represents an additional parameter that can regulate adhesion of and subsequent colonization by viable bacteria. Topographical features can also influence the arrangement behavior of bacteria on substrata which ultimately influences their ability to form biofilms [80]. Under light microscopy, the CDM-modified silicone is observed to exhibit heterogeneously distributed "pockets" of CDM within the polymer matrix (Figure 4). The release of these CDMs from the silicone matrix may form cavities, influencing topographical features of the substratum such as porosity and roughness.

Dynamic mechanical analysis of the CDM-modified coupons showed increasing material stiffness with both CDM concentration and frequency, as shown in Figure 4. This trend was expected, as the increase in silicone stiffness with increasing filler concentration is well documented [81]. These changes in CDM-modified silicone were however statistically insignificant ($p>0.05$).

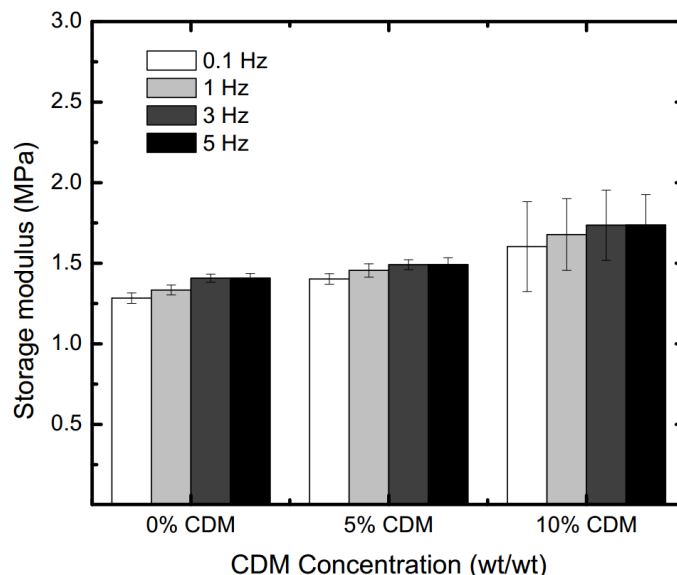


Figure 4: Dynamic mechanical analysis performed on 0, 5 and 10% CDM-modified silicone coupons. Storage modulus is shown to increase with increasing CDM concentration and with increasing frequency, however not significantly.

Elongation at break and ultimate tensile strength were shown to decrease with increasing CDM concentration. This reduction in mechanical performance of the silicone rubber is likely due to the incorporation of the CDM into the polymer matrix. The CDM aggregates could be affecting the alignment of the polymer chains during elongation, leading to breaks at lesser elongation and stress. Contact angle goniometry measurements reported no significant change in contact angle with increasing CDM concentration. This result was unexpected due to the hydrophilic nature of the CDMs, but indicates that the surface hydrophobicity is controlled by the silicone polymer and not the CDM filler.

Table 2: Elongation at break, ultimate tensile strength, and contact angle measurements reported for 0, 5 and 10% CDM-modified coupons. Using a one way ANOVA, no significant change in elongation at break, ultimate tensile strength, and contact angle was found between 0, 5, and 10% CDM modified coupons with $p > 0.05$ in all cases.

CDM wt/wt	Elongation At Break	Ultimate Tensile Strength	Contact Angle
0%	422% \pm 54	4.07 N/mm ² \pm 0.52	109.2° \pm 2.1
5%	387% \pm 24	3.61 N/mm ² \pm 0.09	108.2° \pm 1.4
10%	391% \pm 46	3.38 N/mm ² \pm 0.05	110.2° \pm 1.7

3.3 Biofilm imaging and COMSTAT image analysis

Visual inspection of CLSM images was performed to gain a qualitative assessment of *Proteus mirabilis* biofilm formation on control and CDM-modified coupons. Figure 5a shows 3-dimensional rendering of a biofilm grown on a 0% CDM control coupon. The biofilm comprises mushroom shaped structures which are dense and taller than the surrounding substratum which is absent of micro-colonies. In contrast, biofilms on 5% CDM-modified coupons demonstrate a flattened structure as seen in Figure 5b. Some mushroom structures are visible, but are not as dense nor as tall as those on the control (0%)

coupons. Smaller and more distributed colonies can be identified along the

substratum, demonstrating higher surface coverage of the coupon. Cavitation on the catheter surface (likely from cranberry release) is also observable. These sites are highly fluorescent under confocal microscopy indicating a tendency for cell aggregation and/or biofilm formation in these cavities. Figure 5c depicts biofilms grown on 10% coupons. A complete loss of the

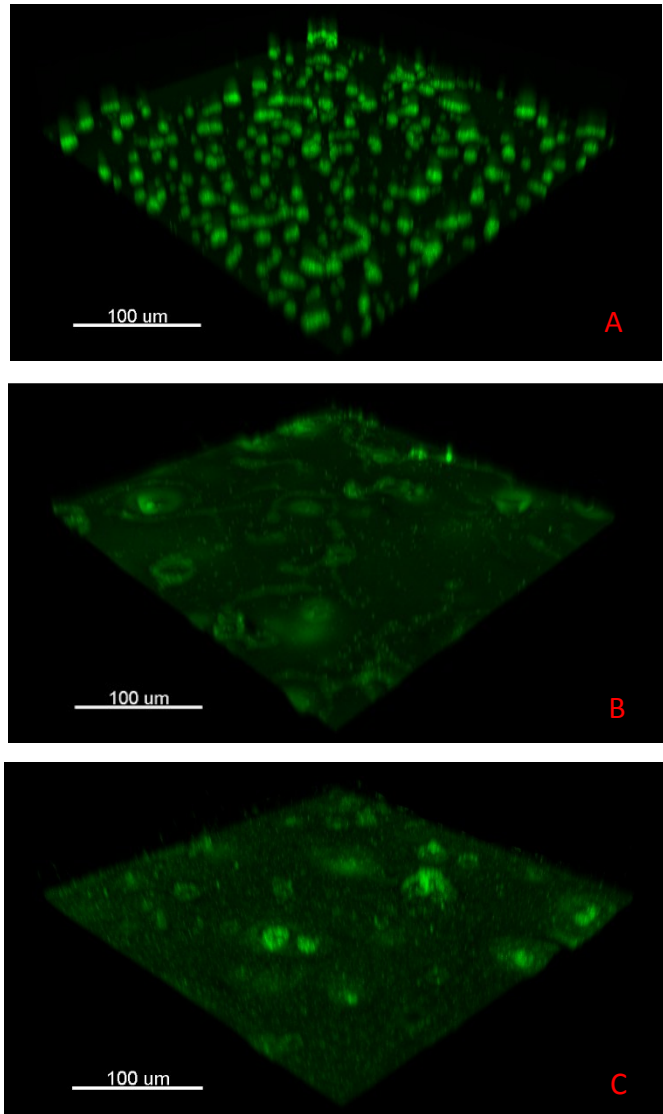


Figure 5: Sample CLSM images of *Proteus mirabilis* biofilms grown on control and CDM-modified silicone over 96 h. 0%, 5%, and 10% CDM coupons are shown in images a, b, and c, respectively.

mushroom structure noted on control (0%) coupons is observed. Multiple small colonies are observable on the silicone substratum, leading to a higher surface coverage. These smaller biofilm colonies are generally less thick than the biofilm structures on the control coupons. Increased cavitation as compared to the 5% CDM coupons is observed, again leading to high concentrations of bacteria in these areas.

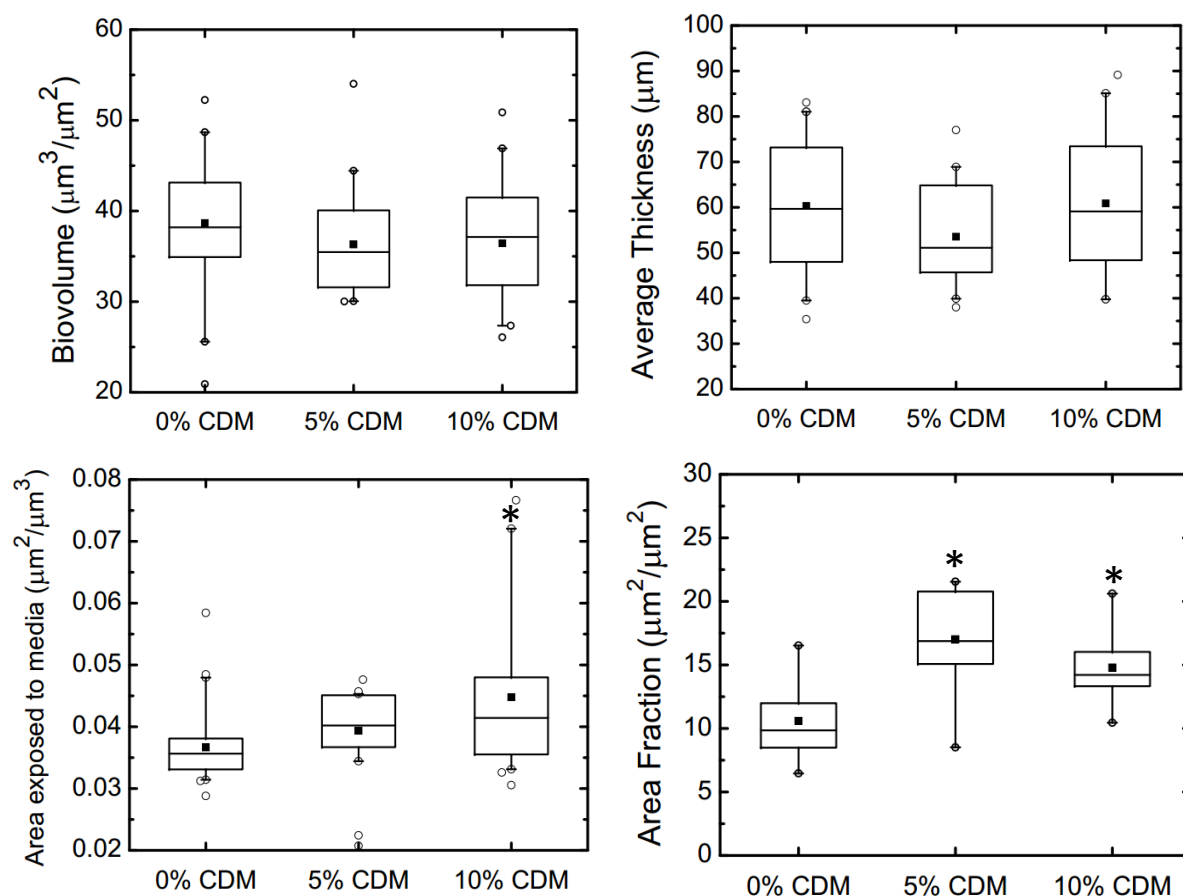


Figure 6: Computational results from COMSTAT 2 image analysis and area fraction measurements by ImageJ. No significant differences in biovolume and average thickness are observed whereas significant differences are observed in regards to area fraction (One-way ANOVA, $[F(2,51)=17.68, p<0.05]$) and area exposed to media (One-way ANOVA, $[F(2,75)=4.56, p<0.05]$). Comparison of CDM coupons to control coupons was performed by *post hoc* t-tests where significance ($p<0.0167$, Bonferroni corrected α) is indicated by (*). Upper and lower box limits represent the top and bottom quartiles, center lines represent the median, (•) represent the average, whiskers represent 5th and 95th percentiles, and (○) represent any outliers.

COMSTAT 2 analysis was performed with purpose of confirming the qualitative analysis of CLSM 3D renderings. COMSTAT 2 biovolume, surface area, and thickness distribution functions were performed on all 81 z-stack images with Otsu's automatic thresholding selected. Biovolume quantification showed no significant difference on 5% and 10% CDM coupons as compared to the 0% CDM control coupons. Average biofilm thickness was extracted from the thickness distribution output from COMSTAT 2. This metric is the average thickness of biofilm across the entire substratum, ignoring the presence of voids. The results demonstrate no significant differences between CDM-modified coupons and the 0% CDM control coupons. The surface area function, with results reported as a surface to volume ratio, was then used to assess the area of biofilm exposed to LB medium. 5% and 10% CDM coupons were shown to have a significantly greater surface to volume ratio as compared to control coupons, which agrees with the qualitative (microscope-based) assessment. Lastly, the area fraction was measured using binary maximum intensity projections of the CLSM images. A significant difference in area fraction between CDM-modified coupons was determined, indicating a greater biofilm surface coverage on cranberry treated coupons.

The biovolume analysis results can be understood by considering that cranberry has not been shown to affect cell growth rates in a planktonic state [40], that there is an observable increase in surface coverage with increasing CDM concentration when examining the CLSM images, and control biofilms visually appear dense compared to CDM coupons and are taller despite covering less of the substratum. Average thickness results are also understandable as there was no significant difference in quantified biovolume despite very different structures observed qualitatively.

3.4 Biofilm disruption, quantification, and viability

The confocal laser scanning microscopy study did not use the propidium iodide component of the BacLight kit due to overlap in the excitation spectrum of PI and some components of the CDM (at 280 nm). Therefore, alternative approaches were used to quantify the number of attached bacteria (to confirm biovolume measurements from CLSM imaging), and to assess bacteria viability via number of colony forming units. Complete biofilm disruption was necessary for enumeration via hemocytometry and CFU/mL; therefore, a series of experiments were conducted with purpose of establishing a reliable method to completely remove biofilm from the silicone substrates. Inspired by Mansouri, Ramanathan [82], a combination of trypsin, scraping using cell scrappers, and sonication was shown to yield acceptable biofilm removal from the silicone substrates. Human serum was added to this method with goal of preserving cell viability by attenuating trypsin enzymatic activity.

The resulting cell suspension was evaluated via hemocytometry, which confirmed the results from CLSM imaging and COMSTAT 2 analysis by showing insignificant differences in number of attached bacteria between control and CDM-modified coupons (Figure 7). Interestingly, plate counts showed a reduction in colony forming bacteria on control coupons as compared to CDM-modified coupons (Figure 7). This result can be explained by the slower metabolism of cells when part of a biofilm community and the lack of nutrient penetration into the thicker and denser biofilm of the control coupons.

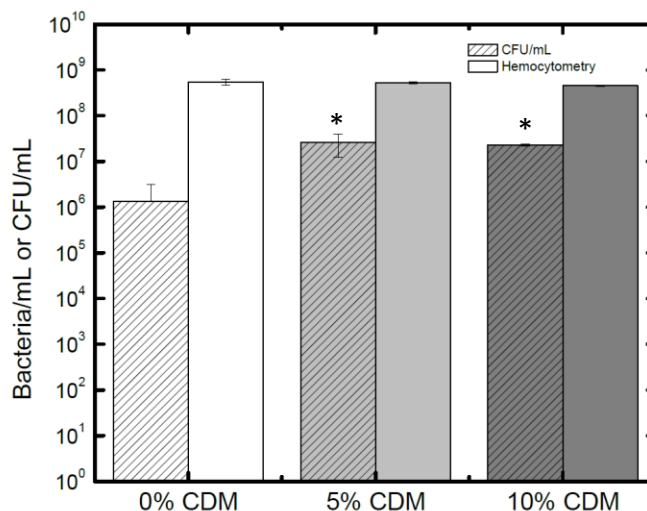


Figure 7: Bacteria/mL and CFU/mL determined via hemocytometry and the Miles and Mistra method, respectively. No significant changes in bacteria count via hemocytometry is observed, however a significant increase ($p < 0.05$) in colony forming units is observed on CDM-modified coupons.

These results demonstrate the ability of CDM to disturb the biofilm formation capability of *Proteus mirabilis* in LB broth. Despite insignificant changes in biovolume, verified via CLSM and hemocytometry, statistically significant changes in visible structure, surface coverage, and surface area exposed to nutrients were observed (albeit minor). The mechanisms by which CDMs influence these *Proteus mirabilis* biofilm characteristics have not been explicitly studied, however previous studies on the effects of motility and nutrient starvation on *P. mirabilis* biofilms can be used to understand these differences. Existing research suggests that swarming motility is not necessary to biofilm formation and that swarming is repressed as exopolysaccharide production is increased [83]. However, the observation of swarmer cells protruding from *P. mirabilis* biofilms was observed via CLSM by Jones et al. [25] and by SEM by Stickler and Morgan [84] suggesting that *P. mirabilis* may differentiate into swarmer cells in an attempt to reach nutrients present within the bulk fluid or to mediate detachment from the biofilm to find new nutrient-rich locations [25]. Since CDMs have been shown to impair

bacterial swarming motility, it can be inferred that biofilm expansion by *P. mirabilis* would subsequently be affected. Jones *et al.* also associated the flat-layer biofilm produced by *P. mirabilis* in urine (as compared to a structured film in LB broth) with nutrient deprivation. This phenomenon was also demonstrated in *Pseudomonas* by Gjermansen et al. [85] where thick structured biofilms starved of carbon reverted to a flat layer with isolated micro-colonies. Although cranberry has not been shown to affect carbon uptake, cranberry proanthocyanidins have been confirmed as iron chelators, forming complexes with ferrous and ferric ions [55]. It is plausible that the chelation of iron by proanthocyanidins may be disrupting the iron acquisition proteins produced by *P. mirabilis*, leading to changes in biofilm formation [55].

Although statistically different results were observed for area fraction, area exposed to media, and cell viability, it is important to note that biofilms were still shown to grow on the CDM-modified silicone surface. Cranberry derived materials can therefore not be recommended as a sole solution to preventing biofilm formation in CAUTIs. However, the change in observed structure via CLSM and the increase in cell viability observed via CFU/mL present the possibility for synergy between cranberry and antibiotic use in the treatment of CAUTI biofilms. The increase in surface area exposed to the aqueous environment would allow for easier diffusion into the biofilm and higher cell viability would likely correlate to higher cell metabolic activity leading to higher rates of antibiotic uptake. The possibility of this synergy is further reinforced by the lower likelihood of antibiotic-resistance gene transfer within the non-structured biofilm.

4. Acknowledgements

This research was supported by NSERC, the Canada Research Chairs Program, and the EUL Fund in the Department of Chemical Engineering at McGill University. The authors would also like to acknowledge Dr. Amir Kamal Miri Ramsheh for his assistance and expertise in the performance of dynamic mechanical analysis experiments.

Chapter 3: Conclusion and Suggested Future Work

This thesis determined the biological and mechanical performance of cranberry modified silicone coupons against the biofilm formation of a common uropathogen, *Proteus mirabilis*. It was hypothesized that the addition of cranberry material into biomedical grade silicone would alter the ability of *P.mirabilis* to form biofilms on the material surface by inhibiting adhesion, motility, and nutrient scavenging mechanisms. Further, it was of interest to study the change in mechanical properties of the silicone due to the addition of the cranberry material into the silicone polymer matrix. The mechanical performance of the hybrid material was first studied, reporting that cranberry modified silicone sustained release of approximately 30% of its cranberry material into a lysogeny broth environment over the course of 96 hours. Further, a positive correlation between CDM concentration and storage modulus was observed, whereas ultimate tensile strength and elongation at break decreased with increasing concentrations of CDM, albeit insignificantly. Moreover, no change in silicone surface hydrophobicity was detected via contact angle goniometry. Bioperformance was then assessed, where the presence of cranberry within the silicone substrate was found to disrupt the structure of *P.mirabilis* biofilms, leading to significant increases in surface coverage and surface exposed to nutrients. Biovolume as reported by COMSTAT 2 and number of bacteria per mL as reported by hemocytometry presented no difference between cranberry modified silicone and controls, whereas *P.mirabilis* viability was found to be higher on cranberry treated silicone.

These results present an interesting case for use of CDM-modified silicone in urinary catheter manufacturing. Although no significant decrease in biovolume was found, the change in biofilm

structure may improve antibiotic performance. Future studies on the role of CDM-modified silicone in CAUTIs should investigate this potential synergy by evaluating the change in minimal inhibitory concentrations of commonly used CAUTI antibiotics. Future studies of the mechanical performance of CDM-modified catheters can also be recommended. Since the ultimate tensile strength and elongation at break have been shown to decrease with increasing CDM concentration (albeit insignificantly), it would be of interest to manufacture a CDM-modified catheter that meets industry standards of mechanical performance.

References

1. Warren, J.W., *Catheter-associated urinary tract infections*. International Journal of Antimicrobial Agents, 2001. **17**(4): p. 299-303.
2. Lo, E., et al., *Strategies to prevent catheter-associated urinary tract infections in acute care hospitals*. Infect Control Hosp Epidemiol, 2008. **29 Suppl 1**(1): p. S41-50.
3. Trautner, B.W., R.A. Hull, and R.O. Darouiche, *Prevention of catheter-associated urinary tract infection*. Curr Opin Infect Dis, 2005. **18**(1): p. 37-41.
4. Scott, RD., *The Direct Medical Costs of Healthcare-Associated Infections in U.S. Hospitals and the Benefits of Prevention*. Division of Healthcare Quality Promotion National Center for Preparedness, Detection, and Control of Infectious Diseases, 2009.
5. Garcia, R., *Prevention of Catheter-Associated UTI: Guidelines and New Insights*. Lecture for CHICA Canada, 2012.
6. Tambyah, P.A., V. Knasinski, and D.G. Maki, *The direct costs of nosocomial catheter-associated urinary tract infection in the era of managed care*. Infect Control Hosp Epidemiol, 2002. **23**(1): p. 27-31.
7. Elvy, J. and A. Colville, *Catheter associated urinary tract infection: what is it, what causes it and how can we prevent it?* Journal of Infection Prevention, 2009. **10**(2): p. 36-41.
8. Gould, C.V., et al., *Guideline for prevention of catheter-associated urinary tract infections*. HICPAC, 2009.
9. Rajesh, K.R., S. Mathavi, and R.I. Priyadarsini, *Prevalence of antimicrobial resistance in uropathogens and determining empirical therapy for urinary tract infections*. International Journal of Basic Medical Science, 2010. **1**(5).
10. Kallen, A., *Multidrug resistance among gram-negative pathogens that caused healthcare-associated infections reported to the NHSN*. ICHE, 2007-2008.
11. Tambyah, P.A., K.T. Halvorson, and D.G. Maki, *A prospective study of pathogenesis of catheter-associated urinary tract infections*. Mayo Clin Proc, 1999. **74**(2): p. 131-6.
12. Kearns, D.B., *A field guide to bacterial swarming motility*. Nat Rev Microbiol, 2010. **8**(9): p. 634-44.
13. Henrichsen, J., *Bacterial surface translocation: a survey and a classification*. Bacteriol Rev, 1972. **36**(4): p. 478-503.
14. Mattick, J.S., *Type IV pili and twitching motility*. Annu Rev Microbiol, 2002. **56**: p. 289-314.
15. McBride, M.J., *Bacterial gliding motility: multiple mechanisms for cell movement over surfaces*. Annu Rev Microbiol, 2001. **55**: p. 49-75.
16. Barford, J. and A. Coates, *The pathogenesis of catheter-associated urinary tract infection*. Journal of Infection Prevention, 2009. **10**(2): p. 50-56.

17. O'Toole, G., H.B. Kaplan, and R. Kolter, *Biofilm formation as microbial development*. Annu Rev Microbiol, 2000. **54**: p. 49-79.
18. Altman, P.L. and D.S. Dittmer, *Blood and Other Body Fluids*. Federation of American Societies for Experimental Biology, 1961: p. 564.
19. Broomfield, R.J., et al., *Crystalline bacterial biofilm formation on urinary catheters by urease-producing urinary tract pathogens: a simple method of control*. J Med Microbiol, 2009. **58**(Pt 10): p. 1367-75.
20. McLean, R.J., et al., *Proteus mirabilis biofilm protection against struvite crystal dissolution and its implications in struvite urolithiasis*. J Urol, 1991. **146**(4): p. 1138-42.
21. Siegfried, L., et al., *Virulence-associated factors in Escherichia coli strains isolated from children with urinary tract infections*. J Med Microbiol, 1994. **41**(2): p. 127-32.
22. Ranjan, K.P., et al., *An approach to uropathogenic Escherichia coli in urinary tract infections*. J Lab Physicians, 2010. **2**(2): p. 70-3.
23. Jacobsen, S.M. and M.E. Shirtliff, *Proteus mirabilis biofilms and catheter-associated urinary tract infections*. Virulence, 2011. **2**(5): p. 460-5.
24. Jacobsen, S.M., et al., *Complicated catheter-associated urinary tract infections due to Escherichia coli and Proteus mirabilis*. Clin Microbiol Rev, 2008. **21**(1): p. 26-59.
25. Jones, S.M., et al., *Structure of Proteus mirabilis biofilms grown in artificial urine and standard laboratory media*. FEMS Microbiol Lett, 2007. **268**(1): p. 16-21.
26. O'May, G.A., et al., *The high-affinity phosphate transporter Pst in Proteus mirabilis HI4320 and its importance in biofilm formation*. Microbiology, 2009. **155**(Pt 5): p. 1523-35.
27. Curtis, J., *A comparative assessment of three common catheter materials*. 2008, Dow Corning Corporation: USA.
28. Colas, A. and J. Curtis, *Silicone Biomaterials: History and Chemistry & Medical Applications of Silicones*. 2nd Edition ed. Biomaterials Science, ed. B. Ratner, et al. 2004, USA: Elsevier Academic Press.
29. Silicone Shin-Etsu, *Characteristic properties of silicone rubber compounds*, Shin-Etsu, Editor. 2005: Japan.
30. Hummer, W. and P. Schreier, *Analysis of proanthocyanidins*. Mol Nutr Food Res, 2008. **52**(12): p. 1381-98.
31. Miles, A.A., S.S. Misra, and J.O. Irwin, *The estimation of the bactericidal power of the blood*. J Hyg (Lond), 1938. **38**(6): p. 732-49.
32. Lai, K.K. and S.A. Fontecchio, *Use of silver-hydrogel urinary catheters on the incidence of catheter-associated urinary tract infections in hospitalized patients*. American Journal of Infection Control, 2002. **30**(4): p. 221-225.

33. Chakravarti, A., et al., *An electrified catheter to resist encrustation by Proteus mirabilis biofilm*. J Urol, 2005. **174**(3): p. 1129-32.
34. Stickler, D.J., et al., *Biofilms on indwelling urethral catheters produce quorum-sensing signal molecules in situ and in vitro*. Applied and Environmental Microbiology, 1998. **64**(9): p. 3486-3490.
35. Girennavar, B., et al., *Grapefruit juice and its furocoumarins inhibits autoinducer signaling and biofilm formation in bacteria*. Int J Food Microbiol, 2008. **125**(2): p. 204-8.
36. Vapnek, J.M., F.M. Maynard, and J. Kim, *A prospective randomized trial of the LoFric hydrophilic coated catheter versus conventional plastic catheter for clean intermittent catheterization*. J Urol, 2003. **169**(3): p. 994-8.
37. Burall, L.S., et al., *Proteus mirabilis Genes That Contribute to Pathogenesis of Urinary Tract Infection: Identification of 25 Signature-Tagged Mutants Attenuated at Least 100-Fold*. Infection and Immunity, 2004. **72**(5): p. 2922-2938.
38. Levering, V., et al., *Soft Robotic Concepts in Catheter Design: an On-Demand Fouling-Release Urinary Catheter*. Adv Healthc Mater, 2014: p. n/a-n/a.
39. O'May, C., et al., *Tannin derived materials can block swarming motility and enhance biofilm formation in Pseudomonas aeruginosa*. Biofouling, 2012. **28**(10): p. 1063-76.
40. O'May, C. and N. Tufenkji, *The swarming motility of Pseudomonas aeruginosa is blocked by cranberry proanthocyanidins and other tannin-containing materials*. Appl Environ Microbiol, 2011. **77**(9): p. 3061-7.
41. Hidalgo, G., M. Chan, and N. Tufenkji, *Inhibition of Escherichia coli CFT073 fliC expression and motility by cranberry materials*. Appl Environ Microbiol, 2011. **77**(19): p. 6852-7.
42. Foo, L.Y., et al., *The structure of cranberry proanthocyanidins which inhibit adherence of uropathogenic P-fimbriated Escherichia coli in vitro*. Phytochemistry, 2000. **54**(2): p. 173-181.
43. Brooks, T. and C.W. Keevil, *A simple artificial urine for the growth of urinary pathogens*. Lett Appl Microbiol, 1997. **24**(3): p. 203-6.
44. Habash, M.B., et al., *Adsorption of urinary components influences the zeta potential of uropathogen surfaces*. Colloids and Surfaces B: Biointerfaces, 2000. **19**(1): p. 13-17.
45. Liu, Y., et al., *Cranberry changes the physicochemical surface properties of E. coli and adhesion with uroepithelial cells*. Colloids Surf B Biointerfaces, 2008. **65**(1): p. 35-42.
46. Ahuja, S., B. Kaack, and J. Roberts, *Loss of fimbrial adhesion with the addition of Vaccinium macrocarpon to the growth medium of P-fimbriated Escherichia coli*. Journal of Urology, 1998. **159**(2): p. 559-562.
47. Foo, L., et al., *A-type proanthocyanidin trimers from cranberry that inhibit adherence of uropathogenic P-fimbriated Escherichia coli*. Journal of Natural Products, 2000. **63**: p. 1225-1228.
48. Delehanty, J.B., et al., *Binding and neutralization of lipopolysaccharides by plant proanthocyanidins*. J Nat Prod, 2007. **70**(11): p. 1718-24.

49. Harmidy, K., N. Tufenkji, and S. Gruenheid, *Perturbation of host cell cytoskeleton by cranberry proanthocyanidins and their effect on enteric infections*. PLoS One, 2011. **6**(11): p. e27267.
50. Gupta, K., et al., *Cranberry products inhibit adherence of p-fimbriated Escherichia coli to primary cultured bladder and vaginal epithelial cells*. J Urol, 2007. **177**(6): p. 2357-60.
51. Di Martino, P., et al., *Reduction of Escherichia coli adherence to uroepithelial bladder cells after consumption of cranberry juice: a double-blind randomized placebo-controlled cross-over trial*. World J Urol, 2006. **24**(1): p. 21-7.
52. Eydelnant, I.A. and N. Tufenkji, *Cranberry derived proanthocyanidins reduce bacterial adhesion to selected biomaterials*. Langmuir, 2008. **24**(18): p. 10273-81.
53. Allison, D.G., et al., *Influence of cranberry juice on attachment of Escherichia coli to glass*. J Basic Microbiol, 2000. **40**(1): p. 3-6.
54. McCall, J., et al., *Cranberry impairs selected behaviors essential for virulence in Proteus mirabilis HI4320*. Can J Microbiol, 2013. **59**(6): p. 430-6.
55. Hidalgo, G., et al., *Induction of a state of iron limitation in uropathogenic Escherichia coli CFT073 by cranberry-derived proanthocyanidins as revealed by microarray analysis*. Appl Environ Microbiol, 2011. **77**(4): p. 1532-5.
56. Tapiainen, T., et al., *Biofilm formation and virulence of uropathogenic Escherichia coli in urine after consumption of cranberry-lingonberry juice*. Eur J Clin Microbiol Infect Dis, 2012. **31**(5): p. 655-62.
57. Feldman, M., et al., *Cranberry proanthocyanidins inhibit the adherence properties of Candida albicans and cytokine secretion by oral epithelial cells*. BMC Complement Altern Med, 2012. **12**: p. 6.
58. LaPlante, K.L., et al., *Effects of cranberry extracts on growth and biofilm production of Escherichia coli and Staphylococcus species*. Phytother Res, 2012. **26**(9): p. 1371-4.
59. Chen CS, et al., *Urine post equivalent daily cranberry juice consumption may opsonize uropathogenicity of Escherichia coli*. J Infect Chemother, 2014. **18**(5): p. 812-817.
60. Feng G, et al., *The specific degree-of-polymerization of A-type proanthocyanidin oligomers impacts Streptococcus mutans glucan-mediated adhesion and transcriptome responses within biofilms*. Biofouling, 2013. **29**(6): p. 629-640.
61. Magill, S.S., et al., *Prevalence of healthcare-associated infections in acute care hospitals in Jacksonville, Florida*. Infect Control Hosp Epidemiol, 2012. **33**(3): p. 283-91.
62. CDC, *Catheter-associated urinary tract infection (CAUTI) Event*. Device-associated module CAUTI, 2014.
63. Denstedt, J., T.A. Wollin, and G. Reid, *Biomaterials used in urology: current issues of biocompatibility, infection, and encrustation*. J Endourol, 1998. **12**(6): p. 493-500.
64. Campos, M.A., et al., *Capsule polysaccharide mediates bacterial resistance to antimicrobial peptides*. Infect Immun, 2004. **72**(12): p. 7107-14.

65. Trautner, B.W. and R.O. Darouiche, *Role of biofilm in catheter-associated urinary tract infection*. Am J Infect Control, 2004. **32**(3): p. 177-83.
66. Hausner, M. and S. Wuertz, *High rates of conjugation in bacterial biofilms as determined by quantitative in situ analysis*. Applied Environmental Microbiology, 1999. **65**(8): p. 3710-3713.
67. Chan, M., et al., *Inhibition of bacterial motility and spreading via release of cranberry derived materials from silicone substrates*. Colloids Surf B Biointerfaces, 2013. **110**: p. 275-80.
68. Mobley, H.L. and J.W. Warren, *Urease-positive bacteriuria and obstruction of long-term urinary catheters*. J Clin Microbiol, 1987. **25**(11): p. 2216-7.
69. Pearson, M.M., et al., *Complete genome sequence of uropathogenic Proteus mirabilis, a master of both adherence and motility*. J Bacteriol, 2008. **190**(11): p. 4027-37.
70. Belas, R., D. Erskine, and D. Flaherty, *Transposon mutagenesis in Proteus mirabilis*. J Bacteriol, 1991. **173**(19): p. 6289-93.
71. Belas, R., D. Erskine, and D. Flaherty, *Proteus mirabilis mutants defective in swarmer cell differentiation and multicellular behavior*. J Bacteriol, 1991. **173**(19): p. 6279-88.
72. Heydorn, A., et al., *Quantification of biofilm structures by the novel computer program COMSTAT*. Microbiology, 2000. **146** (Pt 10): p. 2395-407.
73. <http://www.comstat.dk>.
74. Vorregaard M, et al., *Personal communication*.
75. Nandkumar, A.M., et al., *Antimicrobial Silver Oxide Incorporated Urinary Catheters for Infection Resistance*. Trends Biomater. Artif. Organs., 2010. **24**(3): p. 156-164.
76. Hu, Z., et al., *Controlled release from a composite silicone/hydrogel membrane*. ASAIO J, 2000. **46**(4): p. 431-4.
77. Daneshpour, N., et al., *Indwelling catheters and medical implants with FXIIIa inhibitors: A novel approach to the treatment of catheter and medical device-related infections*. Eur J Pharm Biopharm, 2013. **83**(1): p. 106-13.
78. Pasmore, M., et al., *Effect of Polymer Surface Properties on the Reversibility of Attachment of Pseudomonas aeruginosa in the Early Stages of Biofilm Development*. Biofouling, 2002. **18**(1): p. 65-71.
79. Whitehead, K.A. and J. Verran, *The Effect of Substratum Properties on the Survival of Attached Microorganisms on Inert Surfaces*. Springer Series on Biofilms, 2009. **4**: p. 13-33.
80. Epstein, A.K., et al., *Control of bacterial biofilm growth on surfaces by nanostructural mechanics and geometry*. Nanotechnology, 2011. **22**(49): p. 494007.
81. Fu, S.-Y., et al., *Effects of particle size, particle/matrix interface adhesion and particle loading on mechanical properties of particulate-polymer composites*. Composites Part B: Engineering, 2008. **39**(6): p. 933-961.

82. Mansouri, M.D., et al., *Efficacy of trypsin in enhancing assessment of bacterial colonisation of vascular catheters*. J Hosp Infect, 2010. **76**(4): p. 328-31.
83. Liaw, S.J., H.C. Lai, and W.B. Wang, *Modulation of swarming and virulence by fatty acids through the RsbA protein in Proteus mirabilis*. Infect Immun, 2004. **72**(12): p. 6836-45.
84. Stickler, D.J. and S.D. Morgan, *Modulation of crystalline Proteus mirabilis biofilm development on urinary catheters*. J Med Microbiol, 2006. **55**(Pt 5): p. 489-94.
85. Gjermansen, M., et al., *Characterization of starvation-induced dispersion in Pseudomonas putida biofilms*. Environ Microbiol, 2005. **7**(6): p. 894-906.